



Article

Effects of Humic Acids on the Ecotoxicity of Fe₃O₄ Nanoparticles and Fe-Ions: Impact of Oxidation and Aging

Lyubov Bondarenko ^{1,*}, Anne Kahru ², Vera Terekhova ^{3,4}, Gulzhian Dzhardimalieva ^{1,5}, Pavel Uchanov ⁴ and Kamila Kydralieva ¹

¹ Moscow Aviation Institute, National Research University, 125993 Moscow, Russia; dzhardim@icp.ac.ru (G.D.); KydralievaKA@mai.ru (K.K.)

² Laboratory of Environmental Toxicology, National Institute of Chemical Physics and Biophysics, 12618 Tallinn, Estonia; anne.kahru@kbf.ee

³ Laboratory of Ecotoxicological Analysis of Soil, Faculty of Soil Science, Lomonosov Moscow State University, 119991 Moscow, Russia; vterekhova@gmail.com

⁴ The Laboratory of Ecological Functions of Soil, Institute of Ecology and Evolution, RAS, 119071 Moscow, Russia; p.uchanov@gmail.com

⁵ Laboratory of Metallopolymers, Polymers and Composite Materials Department, Institute of Problems of Chemical Physics RAS, 142432 Chernogolovka, Russia

* Correspondence: BondarenkoLS@mai.ru; Tel.: +7-901-743-3454

Received: 10 September 2020; Accepted: 8 October 2020; Published: 12 October 2020



Abstract: The magnetite nanoparticles (MNPs) are increasingly produced and studied for various environmental applications, yet the information on their ecotoxicity is scarce. We evaluated the ecotoxicity of MNPs (~7 nm) before and after the addition of humic acids (HAs). White mustard *Sinapis alba* and unicellular ciliates *Paramecium caudatum* were used as test species. The MNPs were modified by HAs and oxidized/aged under mild and harsh conditions. Bare MNPs proved not toxic to plants (96 h EC₅₀ > 3300 mg/L) but the addition of HAs and mild oxidation increased their inhibitory effect, especially after harsh oxidation (96 h EC₅₀ = 330 mg/L). Nevertheless, all these formulations could be ranked as ‘not harmful’ to *S. alba* (i.e., 96 h EC₅₀ > 100 mg/L). The same tendency was observed for ciliates, but the respective EC₅₀ values ranged from ‘harmful’ (24 h EC₅₀ = 10–100 mg/L) to ‘very toxic’ (24 h EC₅₀ < 1 mg/L). The ecotoxicity of Fe-ions with and without the addition of HAs was evaluated in parallel: Fe (II) and Fe (III) ions were toxic to *S. alba* (96 h EC₅₀ = 35 and 60 mg/L, respectively) and even more toxic to ciliates (24 h EC₅₀ = 1 and 3 mg/L, respectively). Addition of the HAs to Fe-ions yielded the respective complexes not harmful to plants (96h EC₅₀ > 100 mg/L) but toxic to ciliates (24 h EC₅₀ = 10–100 mg/L). These findings will be helpful for the understanding of the environmental fate and toxicity of iron-based NPs.

Keywords: magnetite nanoparticles; superparamagnetic iron oxide nanoparticles (SPIONs); ferric ions; ferrous ions; humic acids; aging; bioavailability; protozoa; plants; bioassays; aquatic environment; *Sinapis alba*; *Paramecium caudatum*

1. Introduction

Magnetite (Fe₃O₄) is the most magnetic, naturally existing mineral. Along with the development of nanotechnologies, nanosized magnetite has increasingly been produced and studied for applications in various fields from medicine [1] to environmental remediation [2]. For example, Fe₃O₄ nanoparticles (NPs), due to their small size, high surface-area-to-volume ratio, the possibility for surface modification and excellent magnetic properties, have potential in wastewater treatment as magnetically removable

low-cost sorbent carriers for phosphorus [3], heavy metals [4] or photocatalytic particles [5,6]. However, the widespread use of iron oxide nanomaterials will inevitably lead to increased environmental emissions. Thus, the fate and environmental effects of iron oxide nanomaterials must be evaluated [7,8]. Often, commercial NPs are surface-coated to increase their colloidal stability. The latter, however, makes them more motile in an aqueous environment [9]. Moreover, upon release to the environment, the NPs will be transformed being exposed to dissolved oxygen, dissolved organic matter (DOM), various ions, etc. [10]. Thus, the initial physicochemical properties of the magnetite NPs will be altered, depending on environmental compartment they will be released to and assumingly there will be a continuous change in the structure and composition of iron oxide NPs in time, ultimately affecting their bioavailability and toxicity. Thus, bare magnetite NPs are susceptible to air oxidation [11], leading to transformation to other forms of iron oxides [12] and become easily aggregated in aquatic media [13]. Schwaminger et al. [12] simulated the oxidation process of magnetite NPs in harsh (0.07 mol/L HNO₃) and mild (60 °C, air atmosphere) oxidation conditions and showed that in 24 h not only harsh conditions, but also mild conditions led to complete phase transformation of magnetite (Fe₃O₄) to maghemite (γ-Fe₂O₃). In particular, under ambient conditions Fe²⁺ on the surface of Fe₃O₄ NPs tended to rapidly oxidize leading to the transformation of magnetite into maghemite.

The sensitivity to oxygen often limits the use of magnetite NPs, since the particle size, magnetic properties [8], and toxicity will change [10]. Thus, the transformation processes would alter the chemical composition and structure of the NPs and influence their aggregation, dissolution, transport behavior, and even their potential toxicity [14,15]. Lei et al. [10] showed that the inhibition of growth of algae *Chlorella pyrenoidosa* by iron-based NPs decreased with oxidation of the NPs following the order of nZVI > Fe₃O₄ NPs > Fe₂O₃ NPs, whereas the toxicity also depended on the crystal phase as α-Fe₂O₃ NPs were more toxic to algae (96 h EC₅₀ = 71 mg/L) than γ-Fe₂O₃ NPs (96 h EC₅₀ = 132 mg/L). With similar particle size (20–30 nm), iron-based NPs with higher oxidation induced lower oxidative stress and thus lower toxicity to algae [10].

An important role in the fate and transport of iron oxides in the environment plays the humic substances (HS). HS make up the natural organic matter in soils and sediments and are formed from dead organic matter by microbial degradation. HS is divided into three fractions: humic acids, fulvic acids, and humin and can undergo a number of reactions with Fe, e.g., form complexes with both Fe(II) and Fe(III) via carboxyl groups of the organic matter [6]. Also, HS can (i) sorb to iron oxide particles [4] changing their surface charge and affecting their aggregation and bioavailability [16]; (ii) interfere with mineral dissolution/precipitation reactions [17]; and (iii) drive redox reactions [18]. The adsorption of HS to the surface of engineered NPs may strongly influence, and in some cases control, their surface properties and aggregation behavior.

Recent research has shown that humic acids (HA) have a high affinity to Fe₃O₄ NPs and the sorption of HA on the Fe₃O₄ NP enhanced the stability of Fe₃O₄ nanodispersions by preventing their aggregation via electrostatic and steric effects [19–23]. However, weak Coulombic attraction, hydrogen, and hydrophobic (van der Waals, π-π, CH-π) bonds between Fe₃O₄ and HA [24] seemed not to protect Fe₃O₄ NPs from the oxidation in real environmental conditions [25,26]. Thus, redox-active HS play an important role in Fe redox speciation in magnetite and can influence their reactivity and role in biogeochemical Fe cycling. Furthermore, such processes may also influence the fate of other elements bound to the surface of Fe minerals. Redox reactions between HS and the mixed-valent mineral magnetite can potentially lead to changes in Fe (II)/Fe (III) stoichiometry and even dissolve the magnetite [25].

Analyzing the Mössbauer spectroscopy data, Bogart et al. [27] proposed the following mechanism of transformation of Fe₃O₄ to γ-Fe₂O₃ due to the release of Fe-ions from the particles: Fe²⁺ are drawn from the nucleus by a concentration gradient arising due to surface oxidation; Fe²⁺ is oxidized in situ, colliding with mobile electrons, then Fe³⁺ ions are distributed to maintain the electroneutrality of the material. Dissolution of the solid phase and an increase in dissolved Fe²⁺ and/or Fe³⁺ as a result of incubation of NPs with humic substances was demonstrated by Sundman et al. [25]: the magnetite

incubated with native humic substances became more oxidized as compared with the control, i.e., bare magnetite.

Dissolution (shedding of metal ions) as a toxicity mechanism of metal-containing NPs has been extensively studied, especially for some types of NPs, such as nanosilver, ZnO NPs and CuO NPs [28]. For example, Navarro et al. [29] evaluated the toxicity of Ag^+ and AgNPs towards algae *Chlamydomonas reinhardtii* and showed that toxicity of AgNPs to algae was due to shed Ag-ions and particles contributed as a 'carrier' and a source of the Ag-ions. Heinlaan et al. [30] showed that the toxic effects of ZnO and CuO NPs to crustaceans *Daphnia magna* and *Thamnocephalus platyurus* and bacteria *Vibrio fischeri* were due to solubilized Zn^{2+} and Cu^{2+} . The same conclusion was reached for algae *Pseudokirchneriella subcapitata* exposed to ZnO and CuO NPs by Aruoja et al. [31]. Also, Franklin et al. [32] observed that Zn^{2+} ions released from the ZnO NPs were highly toxic to algae *P. subcapitata*.

A meta-analysis of the scientific literature made by Bondarenko et al. [33] covered the (eco)toxicological data for Ag, CuO, and ZnO NPs and respective soluble salts on for algae, crustaceans, fish, bacteria, yeast, nematodes, protozoa and mammalian cell lines. The analysis showed that as a rule, crustaceans, algae and fish proved most sensitive to the studied NPs and at least for AgNPs and ZnO NPs the toxicity was fully explained by solubilized Ag- and Zn-ions, respectively. Analogously, Notter et al. [34] made a meta-analysis of ecotoxicity data for the same types of NPs and the respective metal ions showing that, as a rule, NPs proved less toxic than respective dissolved metal ions. However, to our best knowledge, the information on ecotoxicity of Fe_3O_4 NPs [35] and especially on the contribution of shed Fe-ions to the overall toxicity and effect of humic substances as toxicity modulators [36] is still limited. The current paper aims to fill that gap.

2. Materials and Methods

2.1. Synthesis and Modification of Fe_3O_4 Nanoparticles

2.1.1. Synthesis of Fe_3O_4 and $\text{Fe}_3\text{O}_4/\text{HA}$ Nanoparticles

The bare and humic acid (HA)-coated magnetite nanoparticles (Fe_3O_4 and $\text{Fe}_3\text{O}_4/\text{HA}$ NPs) were synthesized with methods described in [37]. Briefly, a commercial sodium salt of humic acids (HA) (Powhumus, the total acidity of the HA was 5.3 mmol/g of acidic COOH and OH-groups, weight-average molecular weight Mw was 9.9 kD; Humintech, Grevenbroich, Germany) was used for the preparation of $\text{Fe}_3\text{O}_4/\text{HA}$ and other chemicals were from Sigma-Aldrich (Sigma-Aldrich Chemie GmbH, Steinheim, Germany). For the synthesis of NPs, 6.1 g of $\text{FeCl}_3 \cdot 6\text{H}_2\text{O}$ and 4.2 g of $\text{FeCl}_2 \cdot 4\text{H}_2\text{O}$ was dissolved in 100 mL water and heated to 40 °C, then two solutions, 10 mL of ammonium hydroxide (25%), and 0.7 g of HAs were added rapidly and sequentially. The mixture was stirred at 1000 rpm at 40 °C for 10 min under argon atmosphere and then cooled to room temperature. The black precipitate of $\text{Fe}_3\text{O}_4/\text{HA}$ NPs was collected by Nd-magnet (0.3 T) and washed to neutral with distilled water (90 °C) and dried under vacuum at 40 °C. The bare Fe_3O_4 magnetic nanoparticles were synthesized in a similar way, except that no HA was added.

2.1.2. Simulation of Oxidation of $\text{Fe}_3\text{O}_4/\text{HA}$ NPs in Mild and Harsh Conditions

Mild oxidation conditions (aging) were simulated by incubation of the stock aqueous suspensions of $\text{Fe}_3\text{O}_4/\text{HA}$ in the dark at 5 °C for 90 days. Harsh oxidation conditions were simulated by mechanical dispersion of the $\text{Fe}_3\text{O}_4/\text{HA}$ samples in planetary ball mill where the dispersion process takes place between the grinding balls sliding on each other and between the vessel sides and the grinding beads. The $\text{Fe}_3\text{O}_4/\text{HA}$ powder was placed in a wolfram carbide cell with wolfram carbide balls (ball-to-sample mass ratios was 7:1) and dispersed in a high-energy ball mill (SPEX SamplePrep 8000 Mixer/Mill, Metuchen, The Netherlands) at 1425 rpm for 10 min.

2.1.3. Preparation of Complexes of HA with Fe²⁺ and/or Fe³⁺

For the preparation of Fe-HA complexes, a stock solution of the HA (50 mg/L) was prepared by dissolving powdered HA in deionized water with drop-wise addition of 0.1 M NaOH till a final pH = 8. Then, Fe(II) and/or Fe(III) chloride stock solutions (FeCl₂·4H₂O, FeCl₃·6H₂O, 1000 mg/L) were added to HA stock (pH 8.0), to obtain the final ratio HA:Fe(II)/Fe(III) in each series of 1:0.15 according to [38].

Altogether nine different preparations were used for biotesting: aqueous suspensions of Fe₃O₄, Fe₃O₄/HA, HA, soluble salts of Fe³⁺, Fe²⁺, Fe³⁺/Fe²⁺, complexes Fe(II)HA, Fe(III)HA, Fe(II, III)HA. The pH of the suspensions to be tested was adjusted to 7 by diluted HCl and NaOH.

2.2. Characterisation of the Microstructure of Magnetic NPs (MNPs)

The phase composition and primary particle size of the Fe₃O₄, Fe₃O₄/HA and Fe₃O₄/HAox (after oxidation) were determined by X-ray diffraction analysis (XRD) in the Bragg–Brentano geometry using a Philips X-pert diffractometer (Philips Analytical, Eindhoven, The Netherlands, Cr-K α radiation, $\lambda = 2.29106 \text{ \AA}$). The full width at a half maximum (FWHM) of all reflections was used for particle size determination with the Scherrer equation. In order to quantify the oxidation progress, the (440) reflection was fitted with five different functions in Origin 2019 Pro (OriginLab Corporation, Northampton, MA, USA).

The lattice parameters determined for all samples formulated in this study are smaller than those reported for magnetite 8.396–8.400 \AA (ICDD–PDF 19–629), but larger than those for maghemite 8.33–8.34 \AA (ICDD–PDF 39–1346). A plausible explanation of this phenomenon could be the process of partial oxidation of Fe²⁺ during drying and/or storage and modification resulting in the non-stoichiometric Fe_{3- δ} O₄ formation where δ can range from zero (stoichiometric magnetite) to 1/3 (completely oxidized) [39]. For magnetite with an ideal Fe²⁺ content (assuming the Fe₃O₄ formula), the mineral phase is known as stoichiometric magnetite ($x = 0.50$). As magnetite becomes oxidized, the Fe²⁺/Fe³⁺ ratio (formula 4) decreases ($x < 0.50$), with this form denoted as nonstoichiometric or partially oxidized magnetite [39]. The stoichiometry can easily be converted to the following relationship (1):

$$x = \frac{\text{Fe}^{2+}}{\text{Fe}^{3+}} = \frac{1 + 3\delta}{2 + 2\delta} \quad (1)$$

2.3. Characterisation of the Magnetic Properties of Magnetite NPs (MNPs)

Magnetic properties of MNPs dry powders were characterised with Vibrating Sample Magnetometer Lake Shore (Lake Shore Cryotronics, Westerville, OH, USA) at 300 K.

2.4. Analysis of the Surface Charge and Hydrodynamic Diameter of Magnetic NPs (MNPs)

Dynamic light scattering (DLS) measurements were conducted with a “Zetasizer 2c” and “Autosizer 2c” equipment (Malvern Panalytical Ltd., Malvern, UK) at 633 nm with a solid-state He–Ne laser at a scattering angle of 173° at 25 °C. For the DLS analysis, each sample was diluted to approximately 0.1 g/L. Prior to the analysis the magnetic NP suspensions were ultrasonicated for 10 s followed by 100 s of standstill. The average values of the hydrodynamic diameter of NPs were calculated from third-order cumulant fits of the correlation functions using Correlator K7032-09 (Malvern Panalytical Ltd., Malvern, UK). The range of pH was ~7. The experiments were performed at constant ionic strengths 0.01 M set by NaCl.

2.5. Ecotoxicity Testing of Magnetic NPs (MNPs) and Fe-Ions

The toxicity of aqueous suspensions of magnetic NPs towards ciliates was analysed in the concentration range from 0.33 to 33 mg/L and towards plants *Sinapis alba* from 16.5 to 3300 mg/L. The exact concentrations/dilutions tested depending on the test and MNPs and are indicated in the Figures and Tables. The toxicity values (EC₅₀) for MNPs and humic acids (HA) are presented as mg

compound/L (nominal concentrations). Prior testing NP suspensions prepared in distilled water were dispersed by ultrasonication using the sonication bath (100 W, 40 kHz) (Heb Biotechnology, Shaanxi, China) for 10 min.

The exposure concentrations of the Fe^{2+} , Fe^{3+} , $\text{Fe}^{2+}/\text{Fe}^{3+}$ and Fe(II)HA, Fe(III)HA, Fe(II,III)HA used for ecotoxicity testing ranged from 0.149 mg Fe/L to 770 mg Fe/L for ciliates and from 1.49 mg Fe/L to 1540 mg Fe/L for plants. The exact concentrations/dilutions tested depended on the test and compounds. The toxicity values (EC_{50}) for Fe-ions are presented as mg Fe/L.

2.5.1. *Paramecium caudatum* Acute Toxicity Test

The ecotoxicity of magnetic NPs (MNPs) and Fe-ions to ciliates were determined using *Paramecium caudatum* Ehrenberg acute toxicity test performed following the protocol described in [40]. Briefly, the assay is based on the measurement of the mortality of *Paramecium caudatum* when exposed to toxic substances compared with the control. The assay was performed in the 96-well polystyrene plates; well's size 1 mL; Eppendorf). Stock cultures of *P. caudatum* were maintained in the mineral Lozin-Lozinskiy nutrient medium of the following composition, mg/L: NaCl—100.0, KCl—10.0, $\text{CaCl}_2 \cdot 2\text{H}_2\text{O}$ —10.0, $\text{MgCl}_2 \cdot 6\text{H}_2\text{O}$ —10.0, NaHCO_3 —20.0 (Sigma-Aldrich Chemie GmbH, Steinheim, Germany). The stock cultures were maintained at room temperature (22 ± 2 °C), pH 7.5–8.0, without any organic compounds added. To start the test culture, about 1/3 of the stock culture was transferred into a Petri dish containing fresh nutrient medium and incubated at 22 ± 2 °C in the dark for 24 h.

Using a stereoscopic microscope (Model MC-1, Micromed, Shanghai, China), 10–15 ciliates were transferred using a capillary pipette into each of 3–4 test wells containing fresh incubation medium. The volume of liquid when transferring ciliates into the wells did not exceed 0.02 mL. In general, each series of wells (control and test wells) contained at least 30 ciliates. 0.6 mL of incubation medium was added to the control wells; 0.6 mL of the test sample was added to the test wells. The plates with samples and ciliates were incubated at 22 ± 2 °C in the dark. During the exposure period, no food or any other supplements were added. After 24 h of incubation, the individuals were checked for the viability in each well using a stereoscopic microscope. Freely moving ciliates were considered viable, and immobilized individuals were considered dead. The mean values were calculated and compared with the control values.

2.5.2. *Sinapis alba* L. Acute Toxicity Test

The toxicity of MNPs and Fe-ions to plants was measured using the white mustard *Sinapis alba* L. root growth inhibition assay (ISO 18763:2016 [41]) in Phytotoxkit format [42]. Certified, high-quality and commercially available seeds were used for all experiments. Following the Phytotoxkit test format (plate test), the 10 mL of pre-shaken NPs suspension of Fe-ions solutions were poured onto transparent test plates ($21 \times 15.5 \times 0.8$ cm covered by a white filter paper, and ten *Sinapis alba* seeds were placed on the paper. The test plates were closed with a transparent lid and incubated first in a horizontal position at 20 ± 2 °C in darkness for 24 h, and then for 72 h in a vertical position at 24 ± 2 °C and an illumination period of 16 h per day with a light intensity of 4000–7000 lx (light wavelength 400–700 nm, universal white). At the end of the incubation, the length of the main root of the mustard seedlings was measured. The mean values were calculated and compared with the control values. The test was made in three replicates.

2.6. Statistical Analysis

The inhibitory effect of tested compounds/dilutions compared to the control was calculated as a percentage (%). From dose-response curves, the EC_{50} values (mg/L or mg Fe/L, depending on the compound) were calculated using the probit method (IBM SPSS Statistica 17.0, IBM, Armonk, NY, USA) and expressed as an average value \pm standard deviation (SD). ANOVA was used for the analysis of statistically significant variances within and between the test groups. The degree of statistical

significance of the results was calculated in the R-studio application. The programs were created in the programming language R (inter-group statistical significance was fixed at $p \leq 0.05$).

3. Results and Discussion

3.1. Microstructure of Magnetite Nanoparticles (MNPs)

The crystalline structure of the synthesized MNPs was identified using XRD analysis (Figure 1).

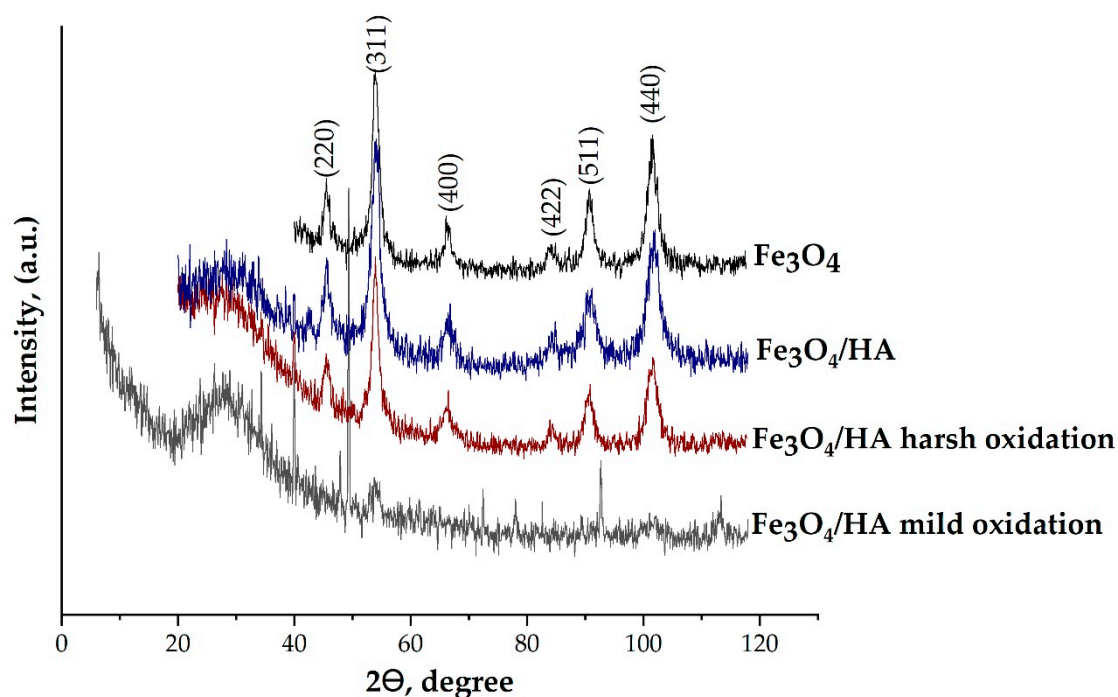


Figure 1. XRD patterns of synthesized Fe_3O_4 nanoparticles. HA—humic acids.

The XRD patterns were similar for all studied NP samples and can be interpreted as a face-centered cubic (fcc) lattice with the parameters of 8.383(2), 8.382(6), 8.365 (5) and 8.250(8) Å for the Fe_3O_4 , $\text{Fe}_3\text{O}_4/\text{HA}$, $\text{Fe}_3\text{O}_4/\text{HA}$ harsh oxidation and $\text{Fe}_3\text{O}_4/\text{HA}$ mild oxidation samples, respectively (Table 1). Finally, the composition of the crystalline component of the pieces can be assigned as follows: $\text{Fe}_{2.94}\text{O}_4$, $\text{Fe}_{2.93}\text{O}_4$ and $\text{Fe}_{2.84}\text{O}_4$ for the Fe_3O_4 , $\text{Fe}_3\text{O}_4/\text{HA}$ and $\text{Fe}_3\text{O}_4/\text{HA}$ harsh oxidation samples, respectively. There was no Fe_3O_4 in the $\text{Fe}_3\text{O}_4/\text{HA}$ sample after mild oxidation in distilled water during 90 days of aging. Magnetite was likely completely oxidized to maghemite and/or other iron species ($\text{Fe}(\text{OH})_3$, FeOOH , etc.). According to [43], the XRD patterns confirm preservation of the spinel structure during oxidation processes: the content of magnetite decreased from ~82.7% to ~79.2%, ~48.3% and 0% for Fe_3O_4 , $\text{Fe}_3\text{O}_4/\text{HA}$ and $\text{Fe}_3\text{O}_4/\text{HA}$ harsh oxidation and $\text{Fe}_3\text{O}_4/\text{HA}$ mild oxidation, respectively (Figure 2).

A slight decrease in the magnetite content in the samples containing humic acids ($\text{Fe}_3\text{O}_4/\text{HA}$) from ~82.7% to ~79.2% (Table 1) can be associated with phenol and quinoid units in the HA structure [44]. Notably, the Fe_3O_4 content in the $\text{Fe}_3\text{O}_4/\text{HA}$ harsh oxidation sample was almost halved, assumingly due to the oxidation of magnetite NPs during mechanical treatment (harsh oxidation). The latter shows that HAs were not forming a strong protective shell to the core interacting mainly via Coulombic attraction and hydrogen bonds. Thus, the magnetite gradually oxidized, producing the increasing maghemite shell after each stage of treatment, i.e., first during the treatment with HA and then during the oxidation in harsh conditions in the high-energy ball mill. Magnetite nanoparticles are seemingly very sensitive to oxygen, and in the presence of air, may undergo oxidation to $\text{Fe}(\text{OH})_3$ [45], or to maghemite ($\gamma\text{-Fe}_2\text{O}_3$) phase. Small amounts of O_2 in water could easily oxidize the Fe^{2+} species to Fe^{3+} , becoming a favorable environment for the production of $\text{Fe}(\text{OH})_3$ or $\gamma\text{-Fe}_2\text{O}_3$. Depending on pH of the

aqueous solution containing Fe^{3+} ions, goethite ($\alpha\text{-FeOOH}$) may be formed due to hydrolysis [46]. Full oxidation of magnetite to maghemite was observed in the case of 90 days of aging in mild condition in the presence of dissolved oxygen. This is coherent with the Tombacz et al. [47], where solid phase transformation of magnetite to maghemite and formation of akageneite shell on the magnetic core after storage at 4 °C for 6 in aqueous medium was observed by XRD analysis.

The step-wise oxidation of magnetite is schematically depicted in Figure 2.

Table 1. Microstructural parameters of synthesized magnetite nanoparticles (MNPs). HA—humic acids.

Sample	Fe_3O_4		$\text{Fe}_3\text{O}_4/\text{HA}$		$\text{Fe}_3\text{O}_4/\text{HA}$ Harsh Oxidation		$\text{Fe}_3\text{O}_4/\text{HA}$ Mild Oxidation	
	hkl	$2\theta, ^\circ$	d, Å	$2\theta, ^\circ$	d, Å	$2\theta, ^\circ$	d, Å	$2\theta, ^\circ$
220	45.60	2.971	45.67	2.966	45.62	2.954861	49.33	2.74502038
311	53.98	2.535	54.01	2.535	53.92	2.526709	53.92	2.52670925
400	66.28	2.094	66.36	2.094	66.39	2.09233	-	-
422	84.25	1.714	84.25	1.714	84.38	1.705695	82.6	1.73564713
511	90.77	1.610	90.71	1.612	90.62	1.61133	92.69	1.58329633
440	101.52	1.476	101.4	1.476	101.68	1.477368	101.3	1.48137719
a, Å	8.383(2)		8.382(6)		8.365(5)		8.250(8)	
x	0.387(7)		0.382(1)		0.232(7)		-	
δ	0.059(4)		0.062(7)		0.154(2)		-	
$\text{Fe}_{3-\delta}\text{O}_4$	$\text{Fe}_{2.94}\text{O}_4$		$\text{Fe}_{2.93}\text{O}_4$		$\text{Fe}_{2.84}\text{O}_4$		-	
% Fe_3O_4	~82.7		~79.2		~48.3		0	
D, nm	6.9 ± 2.4		10.3 ± 1.3		7.8 ± 1.9		11.03 ± 5.1	
CV, %	34		12.6		24.6		50.2	

% Fe_3O_4 is the content of stoichiometric magnetite, CV—coefficient of variation.

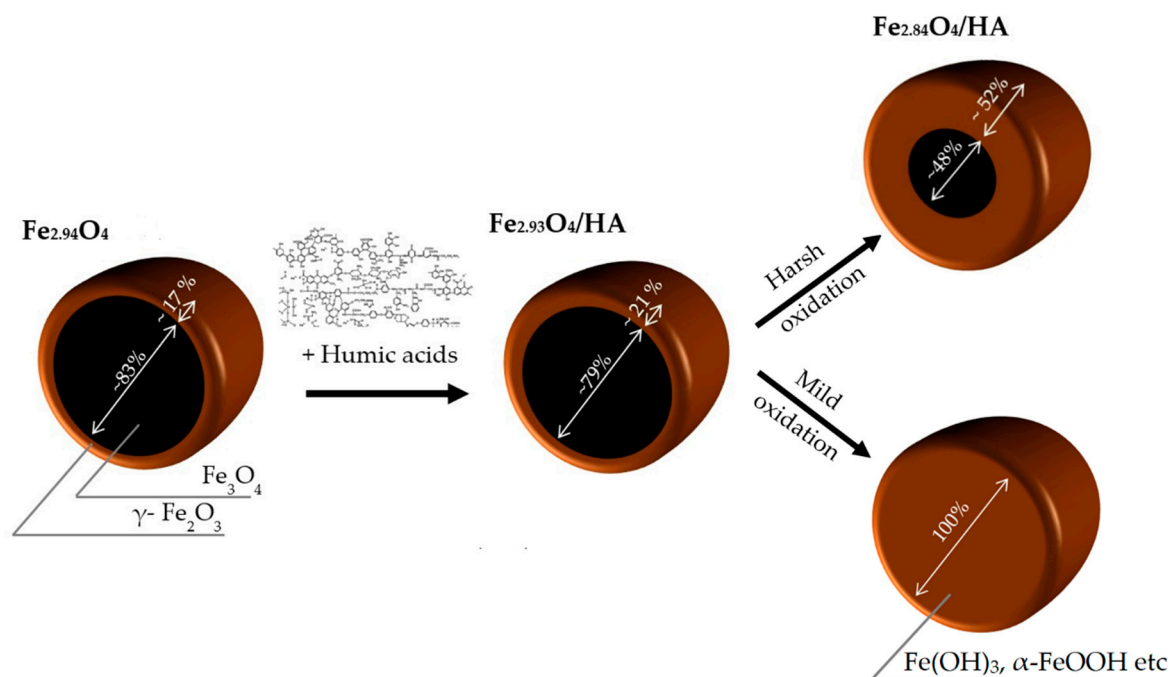


Figure 2. Schematic view of the oxidative transformation of Fe_3O_4 (magnetite; black) to maghemite (Fe_2O_3 ; brown) by treatment with humic acids followed by mild or harsh oxidation. See also Table 1.

The coherent-scattering region size was derived from powder XRD data by Scherrer's method. The full width at half maximum (FWHM) of the reflections was used for particle size determination. In order to quantify oxidation, progress the (440) reflection was fitted with Pseudo-Voigt function for Fe_3O_4 and $\text{Fe}_3\text{O}_4/\text{HA}$ and Voigt function for $\text{Fe}_3\text{O}_4/\text{HA}_{\text{OX}}$ in Origin 2019 Pro. While the spherical

particle shape remained constant for all modification routes, a slight particle growth during modification with HA can be observed (Table 1). The diameter of the bare magnetite particles according to XRD analysis was 6.9 nm, i.e., in the size range of superparamagnetic iron oxide NPs (SPIONs) with a high saturation magnetization and a high specific surface area [48,49]. The diameter for Fe₃O₄/HA particles was 10.3 nm and that of the Fe₃O₄/HA harsh and mild oxidation particles 7.8 and 11.03 nm, respectively. All MNPs were polydisperse [50]. According to the coefficient of variation CV and standard deviation value σ of samples, Fe₃O₄/HA had a smaller size distribution (12.6%, 1.3) than Fe₃O₄ (34%, 2.4), Fe₃O₄/HA harsh (24.6%, 1.9) and mild (50.2%, 5.1) oxidations (Table 1). Therefore, considering the values of CV and σ it could be concluded that in the oxidation process, the primary size for the NPs practically remained unchanged.

3.2. Evaluation of the Magnetic Properties of the Studied MNPs

The most crucial property of magnetite NPs allowing a variety of applications is their ferrimagnetism. Some magnetic characteristics for the Fe₃O₄ MNPs are presented in Table 2. The hysteresis loops are closed and symmetrical versus origin of the coordinate system (Figure S1 in the Supplementary Materials). The shape of the loops evidenced the ferromagnetic character of the material desirable for their application in separation. The respective saturation magnetizations of bare Fe₃O₄ and Fe₃O₄/HA were 68.2 and 30.9 emu/g, respectively, suggesting the content of HA in Fe₃O₄/HA about 40% (w/w). The saturation magnetization for samples of MNPs indicates that magnetite nanoparticles stabilized with humic acids exhibited superparamagnetic properties at room temperature (Figure S1 in Supplementary Materials). The reduced saturation magnetization for Fe₃O₄/HA to 30.9 emu g⁻¹ compared to bare magnetite can be explained by a disordered spin canted structure near the surface of NPs. Our harsh oxidation experiment revealed decreasing to 15.7 emu/g in saturation magnetization as well as changes in the shape of the magnetisation curve (Figure S1). This behavior can be attributed to a change of the composition and to the structure defects arising during oxidation, as shown above by XRD studies (Figure 1). In the absence of a magnetic field, all samples showed a similar low residual magnetism around ± 4 –7 emu g⁻¹ due to magnetic viscosity for superparamagnetic materials [51]. The further increase of the coercivity can be related to an increasing anisotropy by phase transformation to maghemite [52].

Table 2. Magnetic properties of bare, modified and oxidized magnetite NPs.

Sample	Saturation Magnetization Ms, emu/g	Remanent Magnetization Mr, emu/g	Coercive Force Hc, Oe
Fe ₃ O ₄ (bare)	68.2	6.88	74.1
Fe ₃ O ₄ /HA	30.9	6.40	160
Fe ₃ O ₄ /HAox (harsh oxidation)	15.7	4.11	159

HA—humic acids, ox—oxidized.

The black aqueous suspensions of Fe₃O₄/HA nanoparticles were oxidized to brown suspensions after storage in distilled water for 90 days, indicating the HA coating was not able to protect the magnetite from oxidation and to maintain its saturation magnetization. Due to that, the magnetic properties of aged Fe₃O₄/HA were not measured.

3.3. The Ecotoxicity of Bare Fe₃O₄ NPs (MNPs) and Humic Acids-Modified MNPs Before and After Oxidation in Mild and Harsh Conditions

The bare MNPs evaluated for the current study's toxic effects were not toxic to plants *S. alba* in the root length inhibition test: the EC₅₀ value was not reached even at 3300 mg/L (Table 3). Literature data support the not harmful nature of Fe-oxide NPs. For example, Fe₂O₃ NPs were not inhibitory in the seed germination test as at 1000 mg/L 63–104% of the *Lactuca* seeds and 95–100% of the *Raphanus* seeds germinated [53]. Analogously, the magnetite NPs were not toxic to duckweed *Lemna minor*

growth inhibition assay ($EC_{50} > 100$ mg/L) as well as in *Daphnia magna* 48 h immobilization assay ($EC_{50} > 1000$ mg/L) [54].

Table 3. Physicochemical parameters of MNPs and ecotoxicity (EC_{50} *, mg/L) of MNPs and humic acids (HA).

Sample	%Fe ₃ O ₄	ξ , mV	Hydrodynamic Diameter, nm	24 h EC_{50} for <i>P. caudatum</i> , mg/L	96 h EC_{50} for <i>S. alba</i> , mg/L
Fe ₃ O ₄	83	-25.5 ± 6.03	400.8	>33 **	>3300
HA	-	-	-	>33 **	900.65 ± 106.2
Fe ₃ O ₄ /HA	79	-38.8 ± 7.1	153.2	32 ± 3.1	902.71 ± 211.5
Fe ₃ O ₄ /HA harsh oxidation	48	-16.19 ± 2.1	886.7	0.33 ± 0.01	330 ± 10.1
Fe ₃ O ₄ /HA mild oxidation	0 *	-49.63 ± 2.2	586.1	1.40 ± 0.5	951.6 ± 80.2

* EC_{50} is the concentration of a sample reducing the root length or survival of ciliates by 50%; ** highest concentration that was tested; Color code: ≤ 1 mg/L (red) = very toxic; >1 -10 mg/L (orange) = toxic; >10 -100 mg/L (yellow) = harmful; >100 mg/L (green) = "not classified/not harmful". EC_{50} data not allowing ranking are on white background.

The EC_{50} value of bare Fe₂O₃ NPs to ciliates was not reached at the highest tested concentration (33 mg/L) (Table 3). According to Aruoja et al. [55], ciliates *Tetrahymena thermophila* 24 h viability assay yielded an EC_{50} value of 26 mg/L and the 72 h EC_{50} for algae *Pseudokirchneriella subcapitata*, the toxicity of Fe₂O₃ NPs in 72 h growth inhibition assay was 1.9 mg/L. In both cases, the toxicity was not due to the solubilisation of NPs (shedding of Fe-ions).

However, the HA-treated MNPs were more inhibitory to *S. alba* ($EC_{50} \sim 900$ mg/L) than bare MNPs ($EC_{50} > 3300$ mg/L; Table 3), probably due to the effect of humic acids ($EC_{50} \sim 900$ mg/L mg/L). The harsh oxidation (but not the mild oxidation) somewhat increased the toxicity of HA-treated MNPs to plants. Despite that, the EC_{50} values of all these tested compounds were > 100 mg/L and could be considered not harmful (Table 3, Figure 3B).

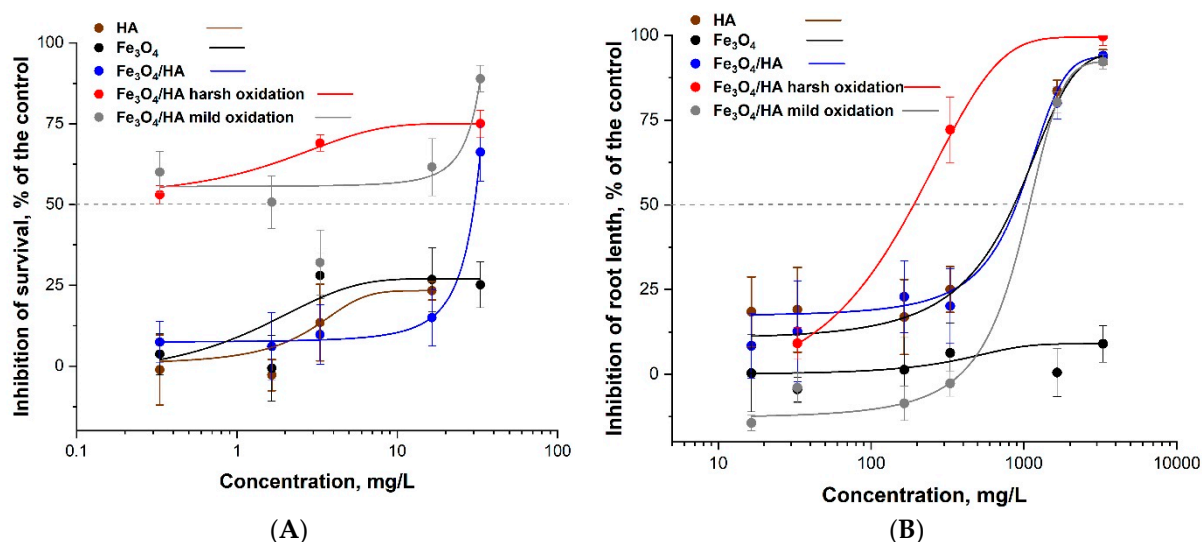


Figure 3. Dose–effect relationships of aqueous suspensions of Fe₃O₄ NPs (MNPs) and MNP-HA complexes before and after harsh and mild oxidation in (A) ciliates *Paramecium caudatum* 24 h immobilization test and (B) higher plants *Sinapis alba* 96 h root growth inhibition test: A dose-effect study. All concentrations are nominal. HA–humic acids. Average values \pm SD of triplicates.

Concerning the effects of MNPs to ciliates, although there was not a very clear dose-effect relationship, the treatment with HAs and following oxidation increased the toxicity of MNPs (Figure 3A). Thus, in general, the trends were similar for plants, but the MNPs, especially after the addition of HAs and following oxidation were remarkably more toxic to ciliates (EC_{50} down to 0.33 mg/L). Thus, the toxicity of iron oxide NPs to ciliates increased in parallel with oxidation of the Fe₃O₄ following the

order: bare Fe_3O_4 < $\text{Fe}_3\text{O}_4/\text{HA}$ < $\text{Fe}_3\text{O}_4/\text{HA}$ mild oxidation < $\text{Fe}_3\text{O}_4/\text{HA}$ harsh oxidation, to *S. alba*: bare Fe_3O_4 < $\text{Fe}_3\text{O}_4/\text{HA}$ mild oxidation < $\text{Fe}_3\text{O}_4/\text{HA}$ < $\text{Fe}_3\text{O}_4/\text{HA}$ harsh oxidation. Summing up, the most toxic compound in both assays were HA-treated MNPs after harsh oxidation (Table 3, Figure 3). The latter may be due to the partial destruction of HAs supramolecule units and released ferrous and ferric ions during harsh mechanical treatment of the $\text{Fe}_3\text{O}_4/\text{HA}$ as ferrous ions are far more toxic than the inherent toxicity of the iron-containing NPs [34]. The reason for the release of the iron ions from $\text{Fe}_3\text{O}_4/\text{HA}$ matrix is probably the supramolecular nature of HA that means associates via weak hydrophobic (van der Waals, π - π , CH- π) and hydrogen bonds [56]. As a result of different treatments (including oxidation), HA can be hydrolyzed, thus leading to the destruction of the protective layer of $\text{Fe}_3\text{O}_4/\text{HA}$. Derivatives of HA contribute to the iron ions release from magnetite. Both iron ions, Fe^{2+} and Fe^{3+} , form strong mixed ligand complexes with HA [57]. Therefore, thermodynamically driven dissolution and subsequent complexation reactions between HA and iron ions can be important for $\text{Fe}_3\text{O}_4/\text{HA}$ dissolution. The dissolution of $\text{Fe}_3\text{O}_4/\text{HA}$ was also confirmed by hydrodynamic particle size analysis via DLS showing a decrease in the particle size [58].

The meta-analysis of the ecotoxicity of NPs made by Juganson et al. [35] described Fe-oxide NPs of relatively low toxicity: the toxicity order for seven types of NPs involved in this study was $\text{Ag} > \text{ZnO} > \text{CuO} > \text{CeO}_2 > \text{CNTs} > \text{TiO}_2 > \text{FeO}_x$ (Fe_2O_3 , Fe_3O_4). Notably, FeO_x NPs had also the lowest amount of available information on their ecotoxicity compared to other above listed NPs and the information on ecotoxicity of FeO_x particles started to emerge in 2009, i.e., later than for the other selected NPs and by the publishing of the paper (2015) there was no data about possible mechanism of action of FeO_x NPs.

3.4. Structure–Bioactivity Relationship for MNPs

Correlating physicochemical properties of studied NPs (primary size, hydrodynamic size, z-potential, percentage of magnetite) and ecotoxicity of MNPs (Table 3, Figure 4) it can be concluded that humic acids can change the toxicity of MNPs in different ways. Importantly, after each step of treatment, whether it be humic acids, harsh oxidation, or 90 days of aging, the percentage of magnetite in MNPs after treatment with HA decreased from 83% to 79% and further to 48% after the harsh oxidation of $\text{Fe}_3\text{O}_4/\text{HA}$ NPs. Interestingly, after mild oxidation of $\text{Fe}_3\text{O}_4/\text{HA}$ the percentage of magnetite fell practically to zero (Table 3). The zeta potentials and hydrodynamic diameters of the above described MNPs also changed reflecting the degree of Fe_3O_4 NPs surface modification by humic acids and hydrolysis of the humic shell during boxidationsn in harsh and mild conditions (Table 3).

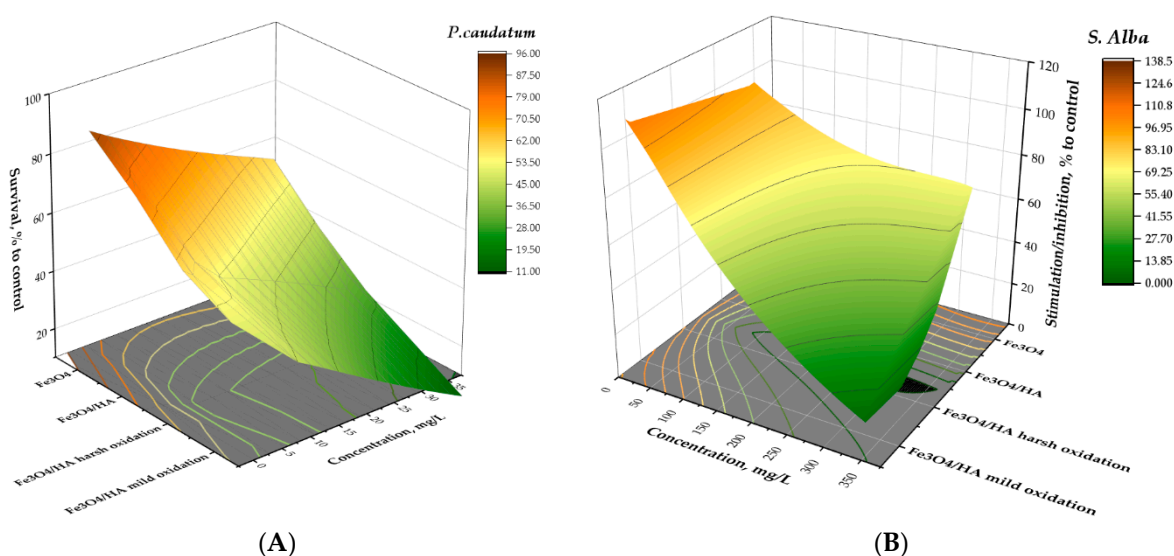


Figure 4. 3D-surface for dependence of toxicity on modification of Fe_3O_4 MNPs; (A) ciliates *Paramecium caudatum* 24 h immobilization test and (B) higher plants *Sinapis alba* 96 h root growth inhibition test: A dose-effect study. All concentrations are nominal.

3.5. The Ecotoxicity of Fe-Ions before and after Addition of Humic Acids

It is still unclear whether the toxicity of iron oxide NPs is specifically related to nanoparticle properties (such as nano-size that also translates into big relative surface area etc.) or is due to the toxicity of shed Fe^{2+} or Fe^{3+} ions, or, both Juganson et al. [35]. Wang et al. [59] studied the toxicity of Fe_2O_3 NPs to bioluminescent bacteria *Photobacterium phosphoreum* and observed EC_{50} value of 200 mg/L (a moderate toxic effect) and showed that the toxic effect was caused solely by NPs and not by shed ions as the NPs were practically nonsoluble. Fe^{3+} ions, however, were very toxic to *P. phosphoreum*, EC_{50} about 0.03 mg Fe/L.

As in the environment the NPs become in contact with humic substances that may affect their behavior and properties, we evaluated the toxicity of Fe_3O_4 -NPs and iron ions (Fe^{2+} and Fe^{3+}) in the presence of humic acids (HA), a natural organic polymer that easily forms complexes with Fe^{2+} and Fe^{3+} and also binds to NPs surface. As test species, plants *S. alba* and ciliates *P. caudatum* were used. The Fe(II, III)-humic complexes and Fe_3O_4 -HA NPs were synthesized as described in Materials and Methods. Test organisms were exposed to: control—culture medium without Fe and HA; samples—Fe(II) or/and Fe(III), HA, Fe(II, III)HA, Fe(II)HA, Fe(III)HA, Fe(II, III)HA.

3.5.1. Ecotoxicity of $\text{Fe}^{2+}/\text{Fe}^{3+}$

As mentioned above, Fe^{3+} ions were very toxic to bioluminescent bacterium *P. phosphoreum*, EC_{50} about 0.03 mg Fe/L [59]. Analogously, Kurvet et al. [60] showed high toxicity of Fe^{3+} ions to another luminescent bacterium, *Vibrio fischeri*, $\text{EC}_{50} = 0.44$ mg/L and EC_{50} of 4.9 mg/L was obtained for ciliates *T. thermophila*. Somewhat lower toxicity of Fe^{3+} ions was shown towards algae *P. subcapitata* ($\text{EC}_{50} = 23$ mg/L) by Aruoja et al. [55].

The current study shows that the EC_{50} values of the Fe-ions to ciliates ranged from 1–3 mg/L whereas Fe^{3+} ions were slightly less toxic than Fe^{2+} ions (Figure 5A) and to *S. alba* from 35–60 mg/L and again, Fe^{3+} ions were slightly less toxic than Fe^{2+} ions (Figure 5B, Table 4). Lower Fe^{3+} toxicity to plants may be due to their lower bioavailability [61] as Fe^{2+} is more soluble and can be more easily absorbed by plants [62]. In general, Fe^{2+} and Fe^{3+} ions were about tenfold more toxic to ciliates than to plants *S. alba*. The mixture of $\text{Fe}^{2+}/\text{Fe}^{3+}$ showed different type of dose-response compared to Fe^{2+} and Fe^{3+} ions separately when exposed to ciliates (Figure 5A), but not in case of *S. alba*. The difference in dose-response may be a result of contribution of several species of ferrous and ferric ions (aqua-ions Fe^{2+} , Fe^{3+} and hydroxocomplexes FeOH^+ , $\text{Fe}(\text{OH})^{2+}$) due to their hydrolysis in biotesting environment used for ciliates.

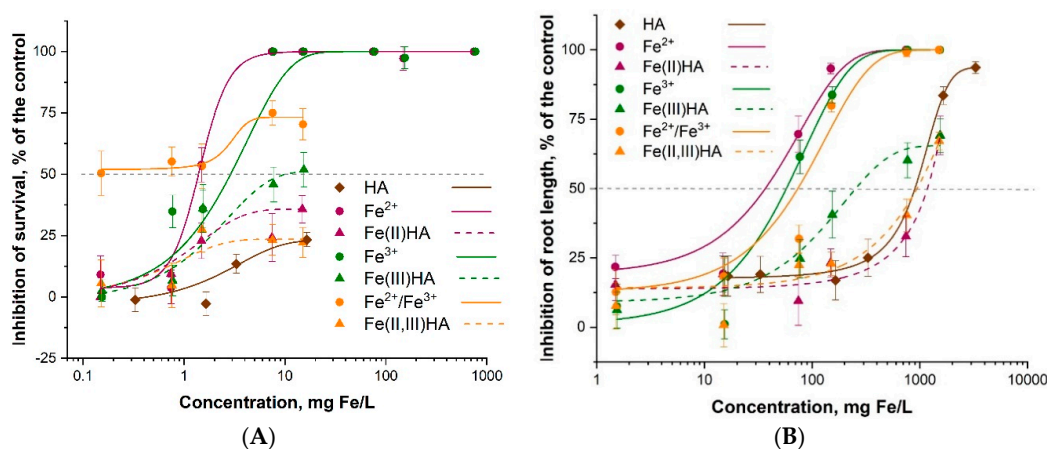


Figure 5. Dose–effect relationships of aqueous suspensions of humic acids (HA) and iron ions with and without the added humic acids (A) in ciliates *Parametium caudatum* 24 h immobilization test and (B) in plants *Sinapis alba* 96 h root growth inhibition test. Average values \pm SD of triplicates. All concentrations are nominal.

Table 4. The toxicity (EC₅₀) of magnetite nanoparticles (MNP)s, humic acids (HA), Fe²⁺ and Fe³⁺ ions and their complexes with HAs to ciliates *P. caudatum* and plants *S. alba*.

Sample	EC ₅₀ ± SD (mg/L)
Toxicity to ciliates <i>P. caudatum</i> (24 h EC ₅₀)	
Fe ²⁺ ^a	1.15 ± 1.4
Fe ³⁺ ^a	3.27 ± 0.8
Fe ²⁺ /Fe ³⁺ ^c	0.48
Fe ₃ O ₄	>33
HA	>33
Fe(II)HA	>33
Fe(III)HA	24.6 ± 9.3
Fe(II,III)HA ^{b,c}	>15.1
Fe ₃ O ₄ /HA ^b	32 ± 3.1
Toxicity to plants <i>S. alba</i> (96 h EC ₅₀)	
Fe ²⁺	35.92 ± 18.6
Fe ³⁺	58.71 ± 21.2
Fe ²⁺ /Fe ³⁺	75.21 ± 44.4
Fe ₃ O ₄ ^c	>3300
HA	900.65 ± 106.2
Fe(II)HA	1402.3 ± 135.1
Fe(III)HA	256.18 ± 50.4
Fe(II,III)HA	910.43 ± 270.1
Fe ₃ O ₄ /HA	902.71 ± 211.5

All concentrations are nominal (mg of compound L⁻¹). Average values ± SD of triplicate; ^a Values calculated with IBM SPSS Statistica using the probit method; ^b Values calculated with R using ANOVA. a-c indicate statistical significance. Values with the same letters (a or b) are not significantly different ($p > 0.05$). Samples with letter “c” have no significantly different at concentrations. EC₅₀ values are calculated as mg/L for Fe₃O₄, HAs and Fe₃O₄/HA and as mg Fe/L for Fe-ions; Color code: ≤1 mg/L (red ■) = very toxic; >1–10 mg/L (orange ■) = toxic; >10–100 mg/L (yellow ■) = harmful; >100 mg/L (green ■) = “not classified/not harmful”. EC₅₀ data not allowing ranking are on white background.

3.5.2. Effects of Humic Acids on the Ecotoxicity of Fe²⁺ and Fe³⁺

The addition of humic acids to iron ions reduced their toxicity to *S. alba* about 10-fold and EC₅₀ values of Fe-HA complexes proved higher than 100 mg/L, i.e., the complexes could be considered not harmful. The same trend was observed in case of toxicity to ciliates: the addition of HA decreased the toxicity of Fe-ions about 10-fold. However, Fe³⁺/HA still remained toxic (EC₅₀ about 25 mg/L) (Figure 5, Table 4). The HA showed also some inhibitory effect to both, ciliates and plants but in general their EC₅₀ values to plants were not exceeding 100 mg/L (Figure 5B) and most probably the same would have been true for ciliates although so high concentration was not tested (Figure 5A).

The addition of humic acids to binary iron solutions lead to a significant reduction in toxicity (EC₅₀ changed from 0.5 to > 100 mg Fe/L) probably due to the formation of chelate-type ternary iron ions humic acids complexes.

Mitigating effect of HA in Fe-ions and HA complexes could be explained by the fact that Fe(II) and Fe(III) are strongly bound to acidic functional groups of HAs [63–67]. It has been reported that complexes of Fe²⁺ and Fe³⁺ with humic acids increased Fe-uptake in plants Garcia [38]. These results are coherent with the fact that after the addition of humic acids Fe²⁺ and Fe³⁺ became less toxic to plants (Table 4). Thermodynamic constants for 1:1 complexes of Fe(III) with weak binding sites in humic substances like carboxylic groups and strong binding sites like phenolic groups are four to 40 times greater than the respective stability constants for Fe(II) complexes [68]. That could be a reason for more pronounced mitigating effect of HA in case of Fe³⁺ (Table 4).

3.6. Acute Toxicity of Fe²⁺/Fe³⁺ with and without Addition of Humic Acids: Effect of Aging

The influence of the aging on the toxicity of HA, Fe²⁺/Fe³⁺ and Fe(II,III)HA was studied using *S. alba* and *P. caudatum* as test species (Table 5, Figure 6). To simulate the aging in mild conditions, the preparations were incubated in water in the dark at 5 °C during 90 days.

In case of ciliates *P. caudatum* (Figure 6A), there were no statistically significant differences in toxicity of as-prepared and aged $\text{Fe}^{2+}/\text{Fe}^{3+}$: both preparations were ‘very toxic’ ($\text{EC}_{50} < 1 \text{ mg/L}$). However, the aging had pronounced effect on toxicity to ciliates in case of humic acids as well as Fe-ions modified with HAs. In both cases the toxicity remarkably increased after aging (Table 5). Interestingly, the toxicity of aged Fe(II,III)HA ($\text{EC}_{50} = 1.4 \text{ mg Fe/L}$) was higher than the toxicity of HA ($\text{EC}_{50} = 1.93 \text{ mg/L}$). The increase of toxicity can be explained by the formulation of hydroxocomplexes of iron ions with humic acids, as well as hydrolysis of humic acids with decomposition into low molecular fractions and fulvic acids, that may affect *P. caudatum*.

For the *S. alba* (Figure 6B), the $\text{Fe}^{2+}/\text{Fe}^{3+}$ proved not toxic before and after aging for 90 days (EC_{50} 75 and 231 mg/L , respectively) and the addition of HAs further decreased their inhibitory effect to plants (EC_{50} of $\text{Fe(II,III)HA} > 900 \text{ mg/L}$) with no remarkable effect of aging ($\text{EC}_{50} = 915 \text{ mg/L}$)(Table 5).

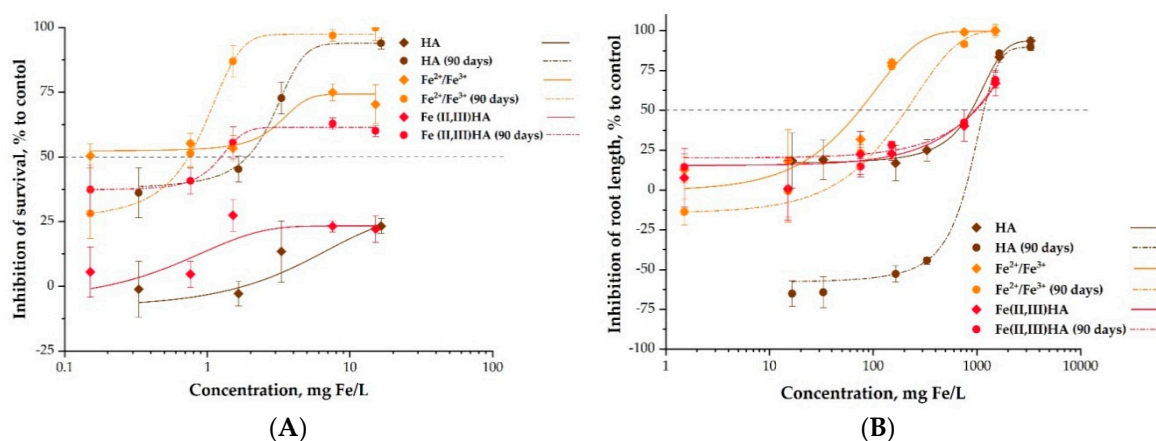


Figure 6. Dose–effect relationships of aqueous suspensions before and after storage (A) in ciliates *Paramecium caudatum* 24 h immobilization test and (B) in plants *Sinapis alba* 96 h root growth inhibition test. Average values \pm SD of triplicates. All concentrations are nominal and concentrations of HA are calculated as mg of HA/L.

Table 5. The toxicity (EC_{50}^a) of humic acids (HA), as prepared and aged $\text{Fe}^{2+}/\text{Fe}^{3+}$ ions to *P. caudatum* and *S. alba*.

Sample	$\text{EC}_{50} \pm \text{SD}$ (mg Fe/L)
Toxicity to ciliates <i>P. caudatum</i> (24 h EC_{50})	
HA *	>33
HA * (90 days)	1.93 \pm 0.55
$\text{Fe}^{2+}/\text{Fe}^{3+}$	0.48 \pm 0.02
$\text{Fe}^{2+}/\text{Fe}^{3+}$ (90 days)	0.67 \pm 0.02
Fe(II,III)HA	>15.1
Fe(II,III)HA (90 days)	1.4 \pm 0.4
Toxicity to plants <i>S. alba</i> (96 h EC_{50})	
HA *	900.65 \pm 106.2
HA * (90 days)	880.1 \pm 123.1
$\text{Fe}^{2+}/\text{Fe}^{3+}$	75.21 \pm 44.4
$\text{Fe}^{2+}/\text{Fe}^{3+}$ (90 days)	231.41 \pm 97.46
Fe(II,III)HA	910.43 \pm 270.1
Fe(II,III)HA (90 days)	915.23 \pm 145.2

All concentrations are nominal (mg of weighed compound L^{-1}). Average values \pm SD of triplicate; ^a Values calculated with IBM SPSS Statistica using the probit method; ^b Values calculated with R using ANOVA; * EC_{50} values for HA are calculated as mg/L; Color code: $\leq 1 \text{ mg/L}$ (red ■) = very toxic; $> 1\text{--}10 \text{ mg/L}$ (yellow ■) = toxic; $>10\text{--}100 \text{ mg/L}$ (yellow ■) = harmful; $> 100 \text{ mg/L}$ (green ■) = “not classified/not harmful”. EC_{50} data not allowing ranking are on white background.

4. Conclusions

In the current study, the magnetite NPs (MNPs) were studied for ecotoxicity (ciliates and plants were used as test species) before and after addition of humic acids, to obtain new scientific information on toxicity of magnetite NPs in environmentally relevant conditions. As Fe-ions maybe shed from MNPs and these ions are far more toxic than MNPs, their toxic effects were studied in parallel. In general, MNPs and Fe-ions were remarkably more inhibitory to ciliates *Paramecium caudatum* than to plants *Sinapis alba*. The MNPs (with or without HA) had no remarkable inhibitory effects to plants *S. alba* even after harsh oxidation (96 h EC₅₀ ~ 300 mg/L). However, Fe-ions were toxic to *S. alba* (EC₅₀ 25–60 mg/L) but the toxic effect was mitigated after addition of HAs.

To ciliates MNPs were toxic whereas the complexing with HAs and aging increased the toxic effects down to 24 h EC₅₀ = 0.33 mg/L after harsh oxidation. The toxicity of Fe-ions to ciliates (EC₅₀ 1–3 mg/L) was reduced after addition of HAs about 10-fold but the complexes still remained toxic to ciliates. Thus, the addition of HAs and aging increased the toxicity of MNPs and mitigated the toxic effect of Fe-ions.

The changes in toxicity were accompanied with the changes in physicochemical properties of MNPs: after each step of treatment as by humic acids, harsh oxidation or 90-days aging the percentage of stoichiometric magnetite decreased from 83 to 79%, to 48%, and to practically to zero, respectively. The zeta potential and hydrodynamic diameter of the above described MNPs also changed reflecting the degree of Fe₃O₄ NPs surface modification by humic acids and hydrolysis of humic shell during both oxidation in harsh and mild conditions.

Supplementary Materials: The following are available online at <http://www.mdpi.com/2079-4991/10/10/2011/s1>, Figure S1. Hysteresis loops at 300 K for Fe₃O₄, Fe₃O₄/HA and Fe₃O₄/HAox; Table S1. Exposure concentration (mg Fe/L) and concentration for soluble Fe-salt and studied MNPs (mg/L); Table S2. *p*-Values calculated with R using ANOVA for the toxicity of MNPs and Fe-ions to *P. caudatum* and *S. alba*; Table S3. *p*-Values for the toxicity (EC₅₀) of humic acids, as prepared and aged Fe²⁺/Fe³⁺ ions to *P. caudatum* and *S. alba*.

Author Contributions: Investigation, software, formal analysis, L.B.; data curation, methodology, writing—original draft preparation, writing—ecotoxicity data interpretation, review and editing, A.K.; resources, investigation of samples microstructure using XRD, magnetic analysis, writing—review and editing, G.D.; experimental studies using biotesting, P.U.; conceptualization, general leadership of the work, data analysis, writing—original draft preparation, writing—review and editing K.K. and V.T. All authors have read and agreed to the published version of the manuscript.

Funding: This research was funded by the Russian Foundation for Basic Research №19-33-90149. Anne Kahru acknowledges the financial support from the European Regional Development Fund project TK134.

Acknowledgments: Gulzhian Dzhardimalieva performed this study in accordance with the state tasks, state registration AAAA-A19-119032690060-9. Vera Terekhova acknowledges the Moscow State University for supporting this work with a grant for Leading Scientific Schools «Depository of the Living Systems» within the framework of the MSU Development Program.

Conflicts of Interest: The authors declare no conflict of interest. The funders had no role in the design of the study; in the collection, analyses, or interpretation of data; in the writing of the manuscript, or in the decision to publish the results.

Abbreviations

HA	Humic acids
HS	Humic substances
NPs	Nanoparticles
MNPs	Magnetite nanoparticles
SPIONs	Superparamagnet iron oxide nanoparticles
XRD	X-ray diffraction analysis
DOM	Dissolved organic matter
nZVI	Nano zerovalent iron
NOM	Natural organic matter
DLS	Dynamic light scattering

References

1. Singh, N.; Jenkins, G.J.; Asadi, R.; Doak, S.H. Potential toxicity of superparamagnetic iron oxide nanoparticles (SPION). *Nano Rev.* **2010**, *1*, 1. [[CrossRef](#)] [[PubMed](#)]
2. Karn, B.; Kuiken, T.; Otto, M. Nanotechnology and in situ remediation: A review of the benefits and potential risks. *Environ. Health Perspect.* **2009**, *117*, 1813–1831. [[CrossRef](#)] [[PubMed](#)]
3. Drenkova-Tuhtan, A.; Mandel, K.; Paulus, A.; Meyer, C.; Hutter, F.; Gellermann, C.; SEXTL, G.; Franzreb, M.; Steinmetz, H. Phosphate recovery from wastewater using engineered superparamagnetic particles modified with layered double hydroxide ion exchangers. *Water Res.* **2013**, *47*, 5670–5677. [[CrossRef](#)] [[PubMed](#)]
4. Bhatia, R.; Singh, R. A review on nanotechnological application of magnetic iron oxides for heavy metal removal. *J. Water. Process Eng.* **2009**, *31*, 100845. [[CrossRef](#)]
5. Xu, P.; Zeng, G.M.; Huang, D.L.; Feng, C.L.; Hu, S.; Zhao, M.H.; Lai, C.; Wie, Z.; Huang, C.; Xie, G.X.; et al. Use of iron oxide nanomaterials in wastewater treatment: A review. *Sci. Total. Environ.* **2012**, *424*, 1–10. [[CrossRef](#)]
6. Yavuz, C.T.; Mayo, J.T.; Yu, W.W.; Prakash, A.; Falkner, J.C.; Yean, S.; Cong, L.; Shipley, H.J.; Kan, A.; Tomson, M.; et al. Low-field magnetic separation of monodisperse Fe₃O₄ nanocrystals. *Science* **2006**, *314*, 964–967. [[CrossRef](#)]
7. Lefevre, E.; Bossa, N.; Wiesner, M.R.; Gunsch, C.K. A review of the environmental implications of in situ remediation by nanoscale zero valent iron (nZVI): Behavior, transport and impacts on microbial communities. *Sci. Total Environ.* **2016**, *565*, 889–901. [[CrossRef](#)]
8. Mahmoudi, M.; Hofmann, H.; Rothen-Rutishauser, B.; Petri-Fink, A. Assessing the in vitro and in vivo toxicity of superparamagnetic iron oxide nanoparticles. *Chem. Rev.* **2012**, *112*, 2323–2338. [[CrossRef](#)]
9. Selmani, A.; Ulm, L.; Kasemets, K.; Kurvet, I.; Erceg, I.; Barbir, R.; Pem, B.; Santini, P.; Delač Marion, I.; Vinković, T.; et al. Stability and toxicity of differently coated selenium nanoparticles under model environmental exposure settings. *Chemosphere* **2020**, *250*, 126265. [[CrossRef](#)]
10. Lei, C.; Zhang, L.; Yang, K.; Zhu, L.; Lin, D. Toxicity of iron-based nanoparticles to green algae: Effects of particle size, crystal phase, oxidation state and environmental aging. *Environ. Pollut.* **2016**, *218*, 505–512. [[CrossRef](#)]
11. Maity, D.; Agrawal, D.C. Synthesis of iron oxide nanoparticles under oxidizing environment and their stabilization in aqueous and non-aqueous media. *J. Magn. Magn. Mater.* **2007**, *308*, 46–55. [[CrossRef](#)]
12. Schwaminger, S.P.; Bauer, D.; Fraga-García, P.; Wagner, F.E.; Berensmeier, S. Oxidation of magnetite nanoparticles: Impact on surface and crystal properties. *CrystEngComm* **2016**, *19*, 246–255. [[CrossRef](#)]
13. Baalousha, M. Aggregation and disaggregation of iron oxide nanoparticles: Influence of particle concentration, pH and natural organic matter. *Sci. Total Environ.* **2009**, *407*, 2093–2101. [[CrossRef](#)] [[PubMed](#)]
14. Lei, C.; Sun, Y.; Tsang, D.C.W.; Lin, D. Environmental transformations and ecological effects of iron-based nanoparticles. *Environ. Pollut.* **2018**, *232*, 10–30. [[CrossRef](#)]
15. Garner, K.L.; Keller, A.A. Emerging patterns for engineered nanomaterials in the environment: A review of fate and toxicity studies. *J. Nanopart. Res.* **2014**, *16*, 2503. [[CrossRef](#)]
16. Tiller, C.L.; O'Melia, C.R. Natural organic matter and colloidal stability: Models and measurements. *Colloids Surf. A Physicochem. Eng. Asp.* **1993**, *73*, 89–102. [[CrossRef](#)]
17. Slowey, A.J. Rate of formation and dissolution of mercury sulfide nanoparticles: The dual role of natural organic matter. *Geochim. Cosmochim. Acta.* **2010**, *74*, 4693–4708. [[CrossRef](#)]
18. Borch, T.; Kretzschmar, R.; Skappler, A.; Van Cappellen, P.; Ginder-Vogel, M.; Voegelin, A.; Campbell, K. Biogeochemical redox processes and their impact on contaminant dynamics. *Environ. Sci. Technol.* **2010**, *44*, 15–23. [[CrossRef](#)]
19. Philippe, A.; Schaumann, G.E. Interactions of dissolved organic matter with natural and engineered inorganic colloids: A review. *Environ. Sci. Technol.* **2014**, *48*, 8946–8962. [[CrossRef](#)]
20. Illés, E.; Tombácz, E. The role of variable surface charge and surface complexation in the adsorption of humic acid on magnetite. *Colloids Surf. A* **2003**, *230*, 99–109. [[CrossRef](#)]
21. Illés, E.; Tombácz, E. The effect of humic acid adsorption on pH-dependent surface charging and aggregation of magnetite nanoparticles. *J. Colloid Interface Sci.* **2006**, *295*, 115–123. [[CrossRef](#)] [[PubMed](#)]

22. Dzhardimalieva, G.I.; Irzhak, V.I.; Bratskaya, S.Y.; Mayorov, V.Y.; Privar, Y.O.; Kasymova, E.D.; Kulyabko, L.S.; Zhorobekova, S.; Kydralieva, K.A. Stabilization of magnetite nanoparticles in humic acids medium and study of their sorption properties. *Colloid J.* **2020**, *82*, 1–7. [[CrossRef](#)]
23. Khundzhua, D.A.; Yuzhakov, V.I.; Korvatovskiy, B.N.; Paschenko, V.Z.; Kulyabko, L.S.; Kydralieva, K.A.; Patsaeva, S.V. Spectroscopic manifestation of interaction of humic acids with trivalent iron ions in aqueous solutions. *Mosc. Univ. Phys. Bull.* **2018**, *73*, 632–637. [[CrossRef](#)]
24. Yurishcheva, A.A.; Dzhardimalieva, G.I.; Kasymova, E.J.; Pomogailo, S.I.; Kydralieva, K.; Li, S.P. The structure of nanocomposites based on magnetite and humic acids produced by chemical coprecipitation and mechanochemical synthesis. *Nanomechanics Sci. Technol. Int. J.* **2014**, *5*, 323–326. [[CrossRef](#)]
25. Sundman, A.; Byrne, J.M.; Bauer, I.; Menguy, N.; Kappler, A. Interactions between magnetite and humic substances: Redox reactions and dissolution processes. *Geochem. Trans.* **2017**, *18*, 1–12. [[CrossRef](#)]
26. Velimirovic, M.; Auffan, M.; Carniato, L.; Micić Batka, V.; Schmid, D.; Wagner, S.; Borschneck, D.; Proux, O.; Von der Kammer, F.; Hofmann, T. Effect of field site hydrogeochemical conditions on the corrosion of milled zerovalent iron particles and their dechlorination efficiency. *Sci. Total Environ.* **2018**, *618*, 1619–1627. [[CrossRef](#)]
27. Bogart, L.K.; Blanco-Andujar, C.; Pankhurst, Q.A. Environmental oxidative aging of iron oxide nanoparticles. *Appl. Phys. Lett.* **2018**, *113*, 133701. [[CrossRef](#)]
28. Kahru, A.; Dubourguier, H.C. From ecotoxicology to nanoecotoxicology. *Toxicology* **2010**, *269*, 105–119. [[CrossRef](#)]
29. Navarro, E.; Piccapietra, F.; Wagner, B.; Marconi, F.; Kaegi, R.; Odzak, N.; Sigg, L.; Behra, R. Toxicity of silver nanoparticles to *Chlamydomonas reinhardtii*. *Environ. Sci. Technol.* **2008**, *42*, 8959–8964. [[CrossRef](#)]
30. Heinlaan, M.; Ivask, A.; Blinova, I.; Dubourguier, H.-C.; Kahru, A. Toxicity of nanosized and bulk ZnO, CuO and TiO₂ to bacteria *Vibrio fischeri* and crustaceans *Daphnia magna* and *Thamnocephalus platyurus*. *Chemosphere* **2008**, *71*, 1308–1316. [[CrossRef](#)]
31. Aruoja, V.; Dubourguier, H.C.; Kasemets, K.; Kahru, A. Toxicity of nanoparticles of CuO, ZnO and TiO₂ to microalgae *Pseudokirchneriella subcapitata*. *Sci. Total Environ.* **2009**, *407*, 1461–1468. [[CrossRef](#)] [[PubMed](#)]
32. Franklin, N.M.; Rogers, N.J.; Apte, S.C.; Batley, G.E.; Gadd, G.E.; Casey, P.S. Comparative toxicity of nanoparticulate ZnO, bulk ZnO, and ZnCl₂ to a freshwater microalga (*Pseudokirchneriella subcapitata*): The importance of particle solubility. *Environ. Sci. Technol.* **2007**, *41*, 8484–8490. [[CrossRef](#)] [[PubMed](#)]
33. Bondarenko, O.; Juganson, K.; Ivask, A.; Kasemets, K.; Mortimer, M.; Kahru, A. Toxicity of Ag, CuO and ZnO nanoparticles to selected environmentally relevant test organisms and mammalian cells in vitro: A critical review. *Arch. Toxicol.* **2013**, *87*, 1181–1200. [[CrossRef](#)] [[PubMed](#)]
34. Notter, D.A.; Mitrano, D.M.; Nowack, B. Are nanosized or dissolved metals more toxic in the environment? *Environ. Toxicol. Chem.* **2014**, *33*, 2733–2739. [[CrossRef](#)] [[PubMed](#)]
35. Juganson, K.; Ivask, A.; Mortimer, M.; Kahru, A. NanoE-Tox: New and in-depth database concerning ecotoxicity of nanomaterials. *Beilstein J. Nanotechnol.* **2015**, *6*, 1788–1804. [[CrossRef](#)] [[PubMed](#)]
36. Walker, H.W.; Bob, M.M. Stability of particle flocs upon addition of natural organic matter under quiescent conditions. *Water Res.* **2001**, *35*, 875–882. [[CrossRef](#)]
37. Pomogailo, A.D.; Kydralieva, K.A.; Zaripova, A.A.; Muratov, V.S.; Dzhardimalieva, G.I.; Pomogailo, S.I.; Golubeva, N.D.; Jorobekova, S.J. Magnetoactive humic-based nanocomposites. *Macromol. Symp.* **2011**, *304*, 18–23. [[CrossRef](#)]
38. Garcia-Mina, J.M.; Sanchez-Diaz, M.; Iniguez, J. The ability of several iron (II)—Humic complexes to provide available iron to plants under adverse soil conditions. In *Iron Nutrition in Soil and Plant*; Abadia, J., Ed.; Kluwer Academic Publishers: Dordrecht, The Netherlands, 1995; pp. 235–239.
39. Gorski, C.A.; Scherer, M.M. Determination of nanoparticulate magnetite stoichiometry by Mossbauer spectroscopy, acid dissolution, and powder X-ray diffraction: A critical review. *Am. Mineral.* **2010**, *95*, 1017–1026. [[CrossRef](#)]
40. Rakhleeva, A.A.; Terekhova, V.A. *Method for Assessment of Toxicity of Wastes, Soil, Sewage Sludge, Surface and Ground Water Using Biotesting Techniques with Paramecium caudatum Ehrenberg (FR. 1.39.2006.02506)*; Moscow University: Moscow, Russia, 2006.
41. ISO 18763:2016. *Soil Quality—Determination of the Toxic Effects of Pollutants on Germination and Early Growth of Higher Plants*; ISO: Geneva, Switzerland, 2016.

42. Nikolaeva, O.V.; Terekhova, V.A. Improvement of laboratory phytotest for the ecological evaluation of soils. *Euras. Soil Sci.* **2017**, *50*, 1105–1114. [CrossRef]
43. Frison, R.; Cernuto, G.; Cervellino, A.; Zaharko, O.; Colonna, G.M.; Guagliardi, A.; Masciocchi, N. Magnetite-maghemite nanoparticles in the 5–15 nm range: Correlating the core-shell composition and the surface structure to the magnetic properties. A total scattering study. *Chem. Mater.* **2013**, *25*, 4820–4827. [CrossRef]
44. Pankratov, D.A.; Anuchina, M.M.; Spiridonov, F.M.; Krivtsov, G.G. Fe₃-δO₄. Nanoparticles Synthesized in the Presence of Natural Polyelectrolytes. *Crystallogr Rep.* **2020**, *65*, 393–397. [CrossRef]
45. Kim, D.K.; Zhang, Y.; Voit, W.; Rao, K.V.; Muhammed, M. Synthesis and Characterization of Surfactant Coated Superparamagnetic Monodispersed Iron Oxide Nanoparticles. *J. Magn. Magn. Mater.* **2001**, *225*, 30–36. [CrossRef]
46. Yamaura, M.; Camilo, R.L.; Sampaio, L.C.; Macêdo, M.A.; Nakamura, M.; Toma, H.E. Preparation and characterization of (3-aminopropyl)triethoxysilane-coated magnetite nanoparticles. *J. Magn. Magn. Mater.* **2004**, *279*, 210–217. [CrossRef]
47. Tombácz, E.; Illés, E.; Majzik, A.; Hajdú, A.; Rideg, N.; Szekeres, M. Ageing in the inorganic nanoworld: Example of magnetite nanoparticles in aqueous medium. *Croat. Chem. Acta.* **2007**, *80*, 503–515.
48. Kolhatkar, A.G.; Jamison, A.C.; Litvinov, D.; Willson, R.C.; Lee, T.R. Tuning the magnetic properties of nanoparticles. *Int. J. Mol. Sci.* **2013**, *14*, 15977–16009. [CrossRef]
49. Roth, H.C.; Schwaminger, S.P.; Schindler, M.; Wagner, F.E.; Berensmeier, S. Influencing factors in the CO-precipitation process of superparamagnetic iron oxide nanoparticles: A model based study. *J. Magn. Magn. Mater.* **2015**, *377*, 81–89. [CrossRef]
50. Romano, F.L.; Ambrosano, G.M.B.; Magnani, M.B.B.; Nouer, D.F. Analysis of the coefficient of variation in shear and tensile bond strength tests. *J. Appl. Oral. Sci.* **2005**, *13*, 243–246. [CrossRef]
51. Laurent, S.; Forge, D.; Port, M.; Roch, A.; Robic, C.; Vander Elst, L.; Muller, R.N. Magnetic iron oxide nanoparticles: Synthesis, stabilization, vectorization, physicochemical characterizations, and biological applications. *Chem. Rev.* **2008**, *108*, 2064–2110. [CrossRef]
52. Baaziz, W.; Pichon, B.P.; Fleutot, S.; Liu, Y.; Lefevre, C.; Greneche, J.M.; Toumi, M.; Mhiri, T.; Begin-Colin, S. Magnetic Iron Oxide Nanoparticles: Reproducible Tuning of the Size and Nanosized-Dependent Composition, Defects, and Spin Canting. *J. Phys. Chem.* **2014**, *118*, 3795–3810. [CrossRef]
53. Ko, K.; Kong, I.C. Toxic effects of nanoparticles on bioluminescence activity, seed germination, and gene mutation. *Appl. Microbiol. Biotechnol.* **2014**, *98*, 3295–3303. [CrossRef]
54. Blinova, I.; Kanarbik, L.; Irha, N.; Kahru, A. Ecotoxicity of nanosized magnetite to crustacean *Daphnia magna* and duckweed *Lemna minor*. *Hydrobiologia* **2017**, *798*, 141–149. [CrossRef]
55. Aruoja, V.; Pokhrel, S.; Sihtmae, M.; Mortimer, M.; Mädlar, L.; Kahru, A. Toxicity of 12 metal-based nanoparticles to algae, bacteria and protozoa. *Environ. Sci. Nano.* **2015**, *2*, 630–644. [CrossRef]
56. Piccolo, A. The supramolecular structure of humic substances: A novel understanding of humus chemistry and implications in soil science. *Adv. Agron.* **2002**, *75*, 57–134. [CrossRef]
57. Kallianou, C.S.; Yassoglou, N.J. Bonding and oxidation state of iron in humic complexes extracted from some Greek soils. *Geoderma* **1985**, *35*, 209–221. [CrossRef]
58. Fujii, M.; Imaoka, A.; Yoshimura, C.; Waite, T.D. Effects of molecular composition of natural organic matter on ferric iron complexation at circumneutral pH. *Environ. Sci Technol.* **2014**, *48*, 4414–4424. [CrossRef] [PubMed]
59. Wang, D.; Lin, Z.; Wang, T.; Yao, Z.; Qin, M.; Zheng, S.; Lu, W. Where does the toxicity of metal oxide nanoparticles come from: The nanoparticles, the ions, or a combination of both? *J. Hazard. Mater.* **2016**, *308*, 328–334. [CrossRef]
60. Kurvet, I.; Juganson, K.; Vija, H.; Sihtmäe, M.; Blinova, I.; Syvertsen-Wiig, G.; Kahru, A. Toxicity of Nine (Doped) Rare Earth Metal Oxides and Respective Individual Metals to Aquatic Microorganisms *Vibrio fischeri* and *Tetrahymena thermophila*. *Materials* **2017**, *10*, 754. [CrossRef] [PubMed]
61. Schulte, E.E. Soil and Applied Iron. Univ. Wisconsin Ext. RP08-2004 (I09/92). Available online: <http://www.soils.wisc.edu/extension/pubs/A3554.pdf> (accessed on 20 July 2020).
62. Briat, J.F. Iron from soil to plant products. *Bull. Acad. Natl. Med.* **2005**, *189*, 1609–1619. [PubMed]
63. Schnitzer, M.; Skinner, S. Organo-metallic interactions in soils: 5. stability constants of Cu⁺⁺, Fe⁺⁺, and Zn⁺⁺-fulvic acid complexes. *Soil Sci.* **1966**, *102*, 361–365. [CrossRef]
64. Van Dijk, H. Cation binding humic acids. *Geoderma* **1971**, *5*, 53–67. [CrossRef]

65. Catrouillet, C.; Davranche, M.; Dia, A.; Bouhnik-Le Coz, M.; Marsac, R.; Pourret, G.; Gruau, G. Geochemical modeling of Fe(II) binding to humic and fulvic acids. *Chem. Geol.* **2014**, *372*, 109–118. [[CrossRef](#)]
66. Fujisawa, N.; Furubayashi, K.; Fukushima, M.; Yamamoto, M.; Komai, T.; Ootsuka, K.; Kawabe, Y. Evaluation of the iron(II)-binding abilities of humic acids by complexometric titration using colorimetry with ortho-phenanthroline. *Humic Subst. Res.* **2011**, *8*, 1–6.
67. Garcia-Mina, J.; Antolín, M.; Sanchez-Diaz, M. Metal-humic complexes and plant micronutrient uptake: A study based on different plant species cultivated in diverse soil types. *Plant. Soil.* **2004**, *258*, 57–68. [[CrossRef](#)]
68. Milne, C.J.; Kinniburgh, D.G.; van Riemsdijk, W.H.; Tipping, E. Generic NICA-Donnan model parameters for metal-ion binding by humic substances. *Environ. Sci. Technol.* **2003**, *37*, 958–971. [[CrossRef](#)] [[PubMed](#)]



© 2020 by the authors. Licensee MDPI, Basel, Switzerland. This article is an open access article distributed under the terms and conditions of the Creative Commons Attribution (CC BY) license (<http://creativecommons.org/licenses/by/4.0/>).